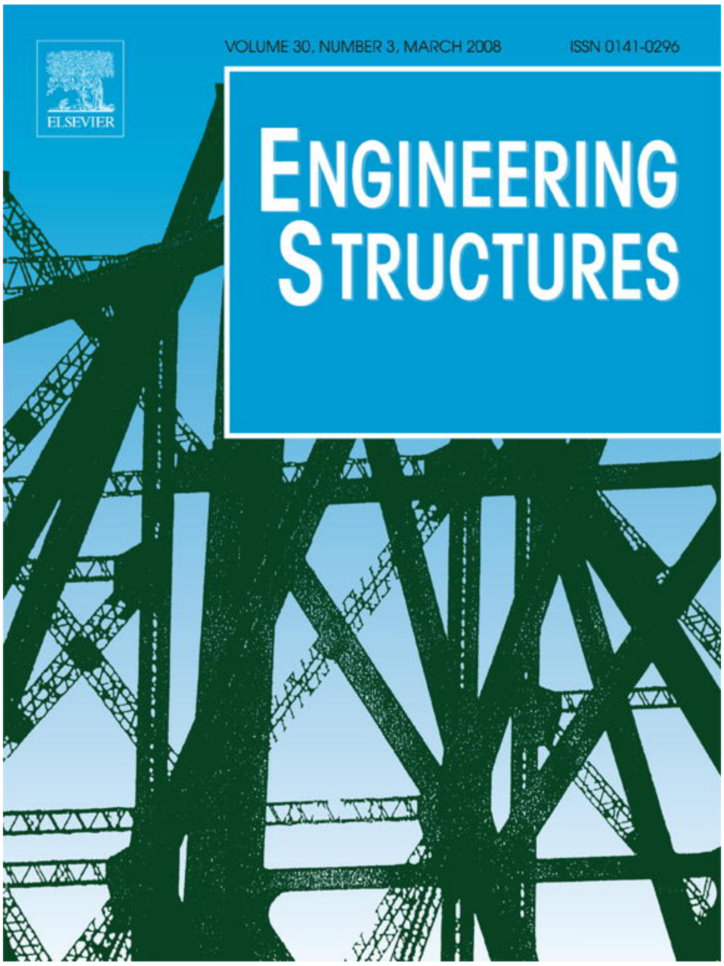
VOLUME 30, NUMBER 3, MARCH 2008
ISSN 0141-0296
ELSEVIER
ENGINEERING STRUCTURES

Available online at www.sciencedirect.com
ScienceDirect
ELSEVIER
Engineering Structures 30 (2008) 794–803
ENGINEERING STRUCTURES
www.elsevier.com/locate/engstruct

Dynamic analysis and seismic performance evaluation of above-ground liquid-containing tanks

Halil Sezen[a,*], Ramazan Livaoglu[b], Adem Dogangun[c]

[a] Department of Civil and Environmental Engineering and Geodetic Science, The Ohio State University, 470 Hitchcock Hall, 2070 Neil Ave., Columbus, OH 43210-1275, United States
[b] Department of Civil Engineering, Karadeniz Technical University, Gümüşhane, Turkey
[c] Department of Civil Engineering, Karadeniz Technical University, Trabzon, Turkey

Received 27 December 2006; received in revised form 30 April 2007; accepted 1 May 2007
Available online 2 July 2007

Abstract

A large number of industrial facilities were damaged during the 1999 M_w7.4 Kocaeli, Turkey earthquake. One of those industrial facilities, Habas plant located within 10 km of the fault trace, provides liquefied gases to commercial plants and medical facilities. Two of the three tanks at the Habas facility collapsed during the earthquake. The main objectives of this paper were to evaluate the seismic performance of tanks and investigate the parameters influencing the dynamic behaviour. Simplified and finite element dynamic analyses of the tanks are carried out including the effect of liquefied gas–structure interaction using a ground motion recorded at a nearby site. The vulnerabilities of the structural system, the observed performance, and damage pattern are discussed by comparing the dynamic analysis results with the strength and deformation capacity of the support columns. The dynamic analysis results from a simplified three-mass model and a finite element model confirmed that the axial and lateral strength of the columns supporting the two nearly full tanks were not sufficient to resist the demand imposed during the earthquake. Consistent with the observed structural performance, an elastic response is predicted for the columns supporting the undamaged 25% full identical tank.

Keywords: Above-ground tanks; Liquefied gas–structure interaction; Sloshing effect; Column failure; Earthquake damage

1. Introduction

The 7.4 magnitude earthquake that struck northwestern Turkey on August 17, 1999 caused extensive damage to residential, commercial, and industrial facilities. Approximately 40% of the heavy industry in Turkey was located in the epicentral region and included oil refineries, pharmaceutical and petrochemical plants, power plants, car assembly and tyre manufacturing facilities, cement production and steel fabrication plants, and other industries. The majority of the affected industrial facilities were located a short distance from the North Anatolian fault that ruptured during the earthquake. Several post-earthquake reconnaissance teams visited the industrial facilities and reported the damages (e.g. Johnson et al. [8]; Rahnama and Morrow [13]; Sezen et al., [14,16]). Structural and non-structural damage to these facilities were summarized and seismic performances were reported using a damage classification scheme by Sezen and Whittaker [15].

The reconnaissance efforts and research studies investigating the performance evaluation of industrial structures during the 1999 Turkey earthquake, for the most part, concentrated on the collapse of a 115 m-high reinforced concrete chimney or heater stack located at the largest oil refinery in Turkey (e.g. Kilic and Sozen [10], and Huang et al. [9]). Seismic analysis and observed behaviour of other industrial structures such as those investigated in this paper provide valuable information in improving the design guidelines for similar new structures as well as performance evaluation of existing structures. The results of this study are particularly important as it evaluates the performance of three identical liquid-containing structures, two of which collapsed while the third one suffered virtually no damage during the earthquake. The only difference between

* Corresponding author.
E-mail addresses: sezen.1@osu.edu (H. Sezen), rliva@ktu.edu.tr (R. Livaoglu), adem@ktu.edu.tr (A. Dogangun).

0141-0296/$ - see front matter © 2008 Published by Elsevier Ltd
doi:10.1016/j.engstruct.2007.05.002

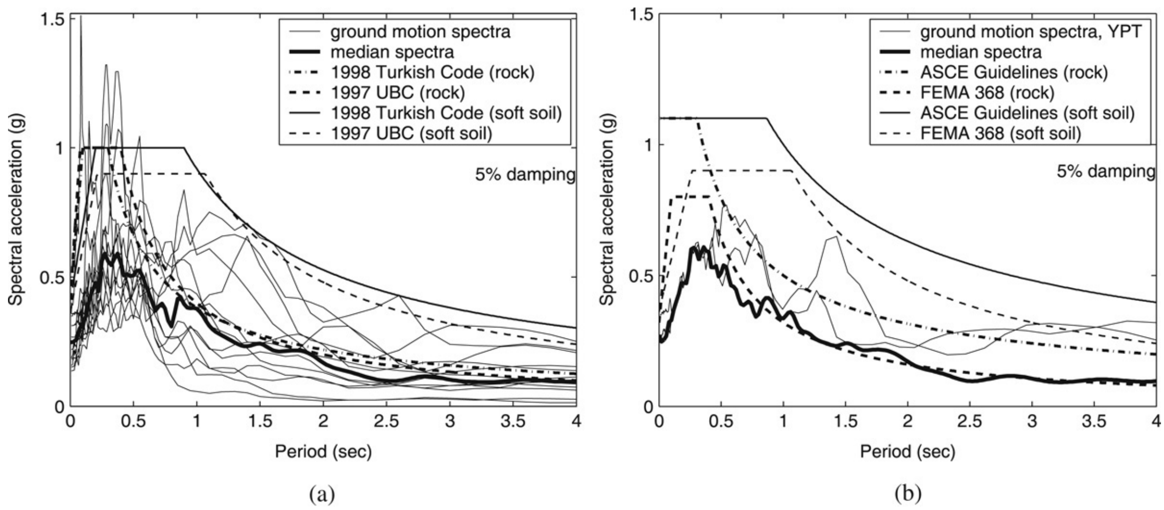

Fig. 1. Elastic ground motion response spectra and design response spectra [15].

Table 1
Recorded peak ground accelerations from stations in epicentral region

Station	Distance[a] (km)	Site class	Peak ground acceleration		
			N-S (%g)	E-W (%g)	Vertical (%g)
Duzce (DZC)	14	Soft soil	37	32	36
Sakarya (SKR)	3	Stiff soil	NA	41	26
Izmit (IZT)	8	Rock	17	22	15
Yarimca (YPT)	4	Soft soil	32	23	24
Gebze (GBZ)	17	Stiff soil	26	14	20
Fatih (FAT)	65	Soft soil	18	16	13
Ambarli (ATS)	79	Soft soil	25	18	8

[a] Distance from rupture plane.

the collapsed and undamaged structures was the amount of the liquefied gas contained inside the tanks. In addition to the obvious effect of increased mass on the dynamic response, the effects of liquefied gas sloshing and liquefied gas–structure interaction are also investigated in this paper.

Modern structural engineering practices aim to prevent shear failure in columns which is brittle and frequently leads to partial or total collapse of the structure. In order to achieve a ductile column response, the shear force, V_p required to develop maximum flexural moment capacity, M_p must be smaller than the shear strength, V_n of the column. For columns bending in double curvature, as in the tanks in this study, $V_p = 2M_p/L$, where L is the total column height and M_p is calculated from moment–curvature analysis using a fiber model for the cross section. The maximum column axial load, bending moment, and shear force demands are calculated from dynamic time history analysis of the empty tank and tanks containing liquefied oxygen and nitrogen. These predicted demands are then compared with the axial load, moment, and shear strength or capacity of the columns.

2. Recorded ground motions and design spectra

The seven strong motion stations that recorded earthquake motions with peak ground accelerations larger than $0.14g$ during the Kocaeli earthquake are listed in Table 1. The closest distance to the fault rupture plane and site classifications are also listed in the table. The elastic response spectra with five-percent damping ratio and the corresponding median spectrum for the 13 horizontal acceleration histories from the seven recording stations are presented in Fig. 1(a). The figure also presents the elastic design spectra calculated using the provisions of the Turkish Seismic Code [18] and the 1997 Uniform Building Code [19] for rock and soft soil sites. The UBC spectra were constructed assuming a near-field amplification factor of 1.0 and soil type S_E (soft soil). Fig. 1(a) can be used to compare the spectral demands from the 13 recorded horizontal ground motions with the elastic demands of the Turkish and US building standards in use at the time of the Kocaeli earthquake. Also shown in the figure is the median spectrum of the 13 horizontal components of ground shaking identified in Table 1.

Two current specifications that can be used for the design of industrial facilities are the *ASCE Guidelines for Seismic Evaluation and Design of Petrochemical Facilities* [2] and *FEMA 368 NEHRP recommended provisions for seismic regulations for new buildings and other structures* [6]. Fig. 1(b) presents the 5% damped ASCE and FEMA 368 elastic spectra and the median spectrum of Fig. 1(a). Based on these data, the earthquake shaking recorded in the epicentral region could be considered as representative of design-basis shaking.

During the 1999 Kocaeli earthquake, Yarimca (YPT) and İzmit (IZT) stations listed in Table 1 were the closest strong motion stations to the Habas plant where the liquefied gas

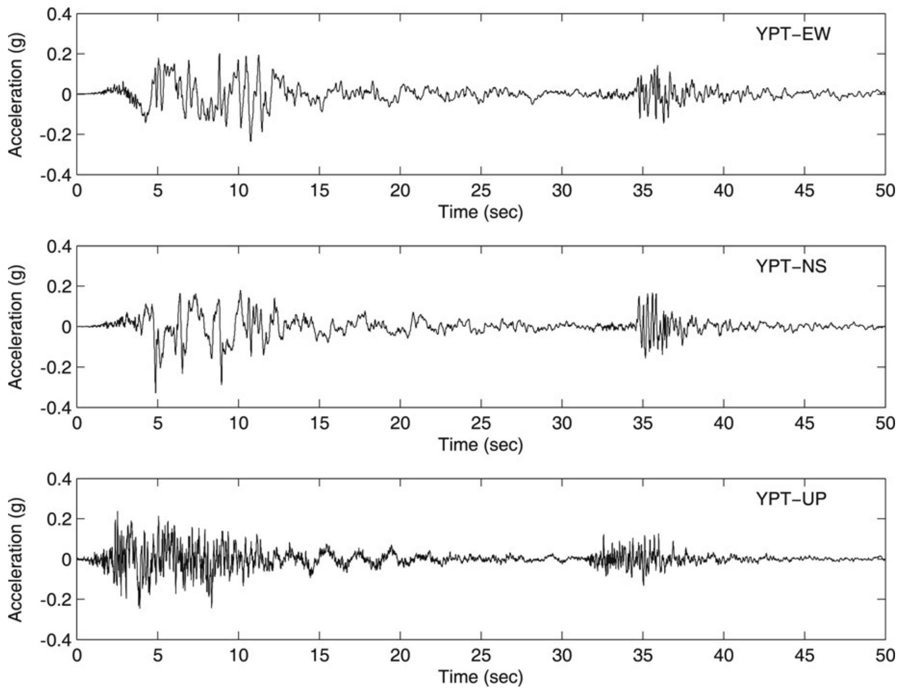

Fig. 2. Ground motions recorded at the YPT station during the 1999 Kocaeli earthquake.

Fig. 3. Two damaged liquefied oxygen tanks (LOXT) and the undamaged liquefied nitrogen tank (LNT, on the right) at the Habas facility.

storage tanks were located. Considering that the site class for Habas was not rock (IZT station was on rock), the earthquake motions recorded at the Yarimca site are used in this paper to analyze the tanks with similar site characteristics. The horizontal (YPT-NS (North–South) and YPT-EW (East–West)) and vertical (YPT-UP) acceleration histories recorded at the YPT station are shown in Fig. 2. The peak horizontal ground acceleration at the YPT station was $0.32g$. In this study, the North–South component of the YPT record is used in the dynamic analysis of the tanks.

3. Description of tanks

The three identical liquefied gas storage tanks at the Habas facility in the Uzunçiftlik area of İzmit, Turkey were built in 1995 (Fig. 3). These tanks, in a sense, are unique structures because they have tall cylindrical vessels supported by relatively short reinforced concrete columns. In traditional elevated tanks or water towers, the vessel is supported by a relatively tall support structure whose dynamic flexural behaviour dominates the overall response. The cylindrical tanks considered herein have geometrical properties similar to those of ground-level tanks, yet their dynamic response is rather different because the total response appears to be largely affected by the dynamic behaviour of support columns.

The two damaged tanks on the left in Fig. 3 contained liquefied oxygen while the undamaged tank on the right had liquefied nitrogen. Habas representatives on site reported that the liquefied oxygen tanks (LOXT) were 85% full and the liquefied nitrogen tank (LNT) was about 25% full immediately before the earthquake. Each tank consisted of two concentric stainless steel shells, one with an outside diameter of 14.6 m and the other with an outside diameter of 12.8 m. The gap between the inner and outer shells was filled with perlite which is a form of natural glass (foam) and a lightweight insulating material. The clear height of the tanks between the bottom slab and top

Fig. 4. Collapsed circular columns under one of the liquefied oxygen tanks.

Fig. 5. Undamaged circular columns supporting the liquefied nitrogen tank.

stainless cover of the tanks is about 12 m. Thus, the volume of the tanks is approximately 1500 m^3. All tanks were supported on a 14.6 m-diameter, 1.07 m-thick reinforced concrete slab that was in turn supported by sixteen 500 mm-diameter reinforced concrete columns. Each column was 2.5 m in height and reinforced with sixteen 16 mm-diameter longitudinal bars and 8 mm-diameter ties spaced at approximately 100 mm on center.

A photograph of some of the failed columns beneath one of the liquefied Oxygen tanks is shown in Fig. 4. Column failures and impact of the tanks to the ground led to buckling of the outer shells of the collapsed tanks. It is estimated that approximately 1200 metric tons of cryogenic liquefied oxygen were released as a result of collapse of the two oxygen storage tanks. The liquefied nitrogen tank next to the collapsed tanks was undamaged except for some hairline cracks in the columns (Fig. 5). The physical properties of structural and contained materials considered in this study are provided in Table 2.

Table 2
Material properties used in the analysis

Physical properties	Material	Moduli or density
Young's modulus	Reinforced concrete	32,000 MPa
	Steel	200,000 MPa
Weight density	Reinforced concrete	25.00 kN/m^3
	Steel	78.50 kN/m^3
	Liquid oxygen (LOX)	11.50 kN/m^3
	Liquid nitrogen (LN)	8.50 kN/m^3
Bulk modulus	Liquid oxygen (LOX)	1200 MPa
	Liquid nitrogen (LN)	1200 MPa

4. Dynamic analysis of tanks

The finite element program, ANSYS [1] with fluid–structure interaction analysis capabilities was used for the dynamic transient time history analysis of the tank systems. In the program, frame elements with six degree-of-freedom per node were used to model the reinforced concrete columns. Quadrilateral four-node-shell elements with six degree-of-freedom per node were used for stainless steel tank walls and eight-node-solid elements with three degree-of-freedom per node were used to model the thick reinforced concrete tank slab. Since the insulating foam material had low stiffness and weight, the filling material between the walls was not included in the computer models. It was assumed that the columns were fixed at the bottom. Fluid inside the tank was modelled with eight-node-brick fluid elements. Such fluid elements in ANSYS are specially formulated to model the fluid contained within a vessel without net flow rate.

Fluid–structure interaction can be modelled using different approaches such as added mass, finite element model (FEM) incorporating Lagrangian, Eulerian, and Lagrangian–Eulerian [4] formulations, or other simplified analytical methods such as two mass representation [7], multi mass representation [3] or the Eurocode-8 method [5]. A comparison and evaluation of these methods are presented by Livaoglu and Dogangun [11]. In this study, a displacement based Lagrangian approach including the effect of liquefied gas–structure interaction is adopted.

The nearly full liquefied oxygen tanks and quarter full liquefied nitrogen tank were analysed to predict the dynamic response under the recorded representative ground motion (Fig. 2). The only difference between the two tank models is the type and amount of liquefied gas contained in the tanks. Considering the liquefied gas–structure interaction, the effect of three selected parameters on the overall behaviour of tanks was investigated. These general parameters included: (a) sloshing displacement of the fluid inside the tanks, (b) lateral displacements at the roof level (top of tanks) and at the top of support columns (bottom of rigid tank slab), and (c) internal forces in columns.

The sloshing displacement of the fluid is important at the service level and for the design of tank roofs. Its effect on the dynamic response appears to be less significant compared to the other response parameters. Therefore, the sloshing effect is sometimes ignored in the simplified analysis. The calculated lateral displacement histories at the selected locations are evaluated to assess the impact of contained fluid on the overall structural performance. Finally, the calculated column internal forces including axial load, shear forces and bending moments are reported. The objective was to compare the axial, shear, and moment strength or capacity of the columns with the internal force demands predicted from dynamic analysis.

4.1. Sloshing displacement

The tanks containing the liquefied oxygen and nitrogen (LOXT and LNT) were analysed considering the effect of

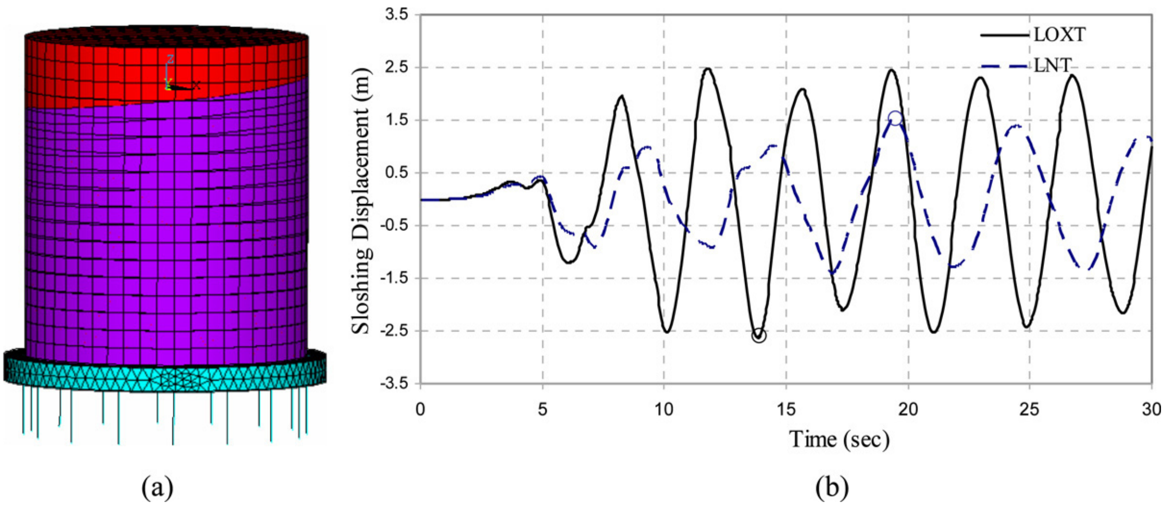

Fig. 6. (a) liquefied oxygen tank model showing the sloshing effect, and (b) calculated sloshing displacement histories.

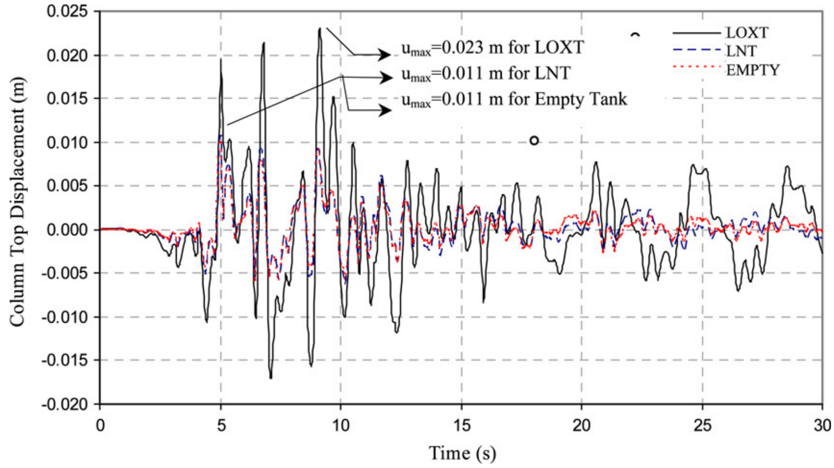

Fig. 7. Calculated displacement time histories at the top of columns.

sloshing on the dynamic response. Fig. 6(b) shows the calculated sloshing response or the variation of liquid level in the vertical direction during the earthquake. The maximum increase in the liquid level due to sloshing in the oxygen and nitrogen tanks were 2.63 m (at 13.85 s) and 1.51 m (at 19.50 s), respectively. As shown in Fig. 6(a), when the sloshing displacement in the oxygen tank reached its maximum, there was sufficient vertical clearance not to affect the tank's roof during the earthquake.

In this research, the effect of liquefied gas sloshing is included in the models, which in turn resulted in time consuming and computationally expensive dynamic analysis. In some simplified analysis, the sloshing of the liquid, hence the effect of convective mass is ignored. In order to investigate the effect of sloshing on the response of the tanks considered here, the liquefied Oxygen is assumed as a rigid solid block without convective mass, and the above dynamic analysis is repeated. It was found for this tank that, if the sloshing effect was ignored, all response quantities were overestimated. For example, the increase in the maximum lateral displacement at the roof level was 25 percent (from 24 to 30 mm) when the sloshing effect was neglected. Similarly, the maximum column shear forces and bending moments increased by 23 percent (from 464 to 572 kN, and 1159 to 1427 kN m) when the sloshing was not considered in the model.

4.2. Lateral displacements

The calculated lateral displacements at the top of columns supporting the empty tank, nearly full oxygen tank, and 25% full nitrogen tank are plotted in Fig. 7. The predicted displacement histories indicate that the dynamic responses of the empty tank and nitrogen tank are similar, with a maximum roof displacement of 11 mm at approximately 5.0 s. A maximum column displacement of 23 mm is predicted for the Oxygen tank at 9.15 s. Thus, the calculated maximum column displacement demand for the Oxygen tank is more than twice larger than that for the nitrogen tank or empty tank.

Fig. 8 shows the lateral displacement distribution over the height of tanks at the maximum calculated displacement. The displacement distribution shows that almost all lateral deformations take place within the 2.5 m high support columns as the vessel itself is relatively rigid and the overturning effects do not seem to contribute significantly to lateral displacements.

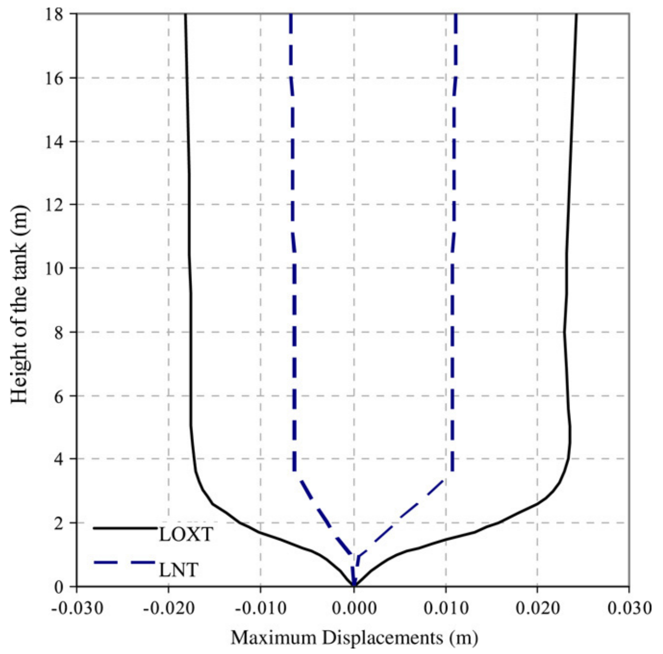

Fig. 8. Lateral displacement distribution over the height of liquefied oxygen tank, LOXT (at 9.15 s) and liquefied nitrogen tank, LNT (at 5.0 s).

The lateral drift demands for the columns supporting the oxygen and nitrogen tanks are then approximately 1.0% and 0.4%, respectively. Consistent with the conclusions drawn from the maximum displacement distributions presented in Fig. 8, the entire time histories of calculated roof displacements for the three tanks were very similar to those shown in Fig. 7. The maximum dynamic roof displacements for the empty tank and tanks containing liquefied nitrogen and oxygen were 11, 11, and 24 mm, respectively.

4.3. Internal forces

The flexural, shear and deformation capacity and the failure mode (ductile or brittle) of a column is associated with the magnitude of the applied axial load and its variation during an earthquake. Failure of one or few columns may lead to partial or total collapse of the structure, as experienced by the liquefied oxygen tanks at the Habas facility. The calculated dynamic axial load histories are presented for the oxygen, nitrogen and empty tanks in Fig. 9. The magnitude of static axial load or the initial gravity load on each column supporting the liquefied oxygen, nitrogen and empty tanks was 1761, 842, and 680 kN, respectively. The maximum axial loads obtained from dynamic analysis including the sloshing and overturning effects are 2648, 1028, and 888 kN as shown in Fig. 9. These maximum dynamic loads represent 50% and 18% increase over the static axial loads in columns supporting the liquefied oxygen and nitrogen tanks.

The flexural demand imposed on the columns is another critical parameter for determining the failure mode and the likely reason for the failure of columns supporting the tanks containing liquefied Oxygen. The calculated dynamic time history of moment demands are shown in Fig. 10. The maximum moment was reached at approximately 9.50 s in columns under each tank. The maximum moment in columns supporting the liquefied oxygen tank is about twice as large as that in other columns.

Some of the collapsed columns at Habas showed signs of apparent shear distress at failure (Fig. 4). When column failures occur under seismic loading, it is imperative to compare the estimated shear force demands with the column shear strength. The predicted dynamic column shear forces or demands are shown in Fig. 11 for the column subjected to maximum shear forces. It appears that the maximum column shear force for the liquefied Oxygen tank is approximately two times larger than that for the empty and liquefied nitrogen tanks.

5. Strength and displacement capacity of columns and comparison with observed response

To better evaluate the seismic performance of the columns supporting the tanks, shear strength and flexural deformation capacities of a sample column are calculated. According to Turkish Standard Code, TS 500 [17], the nominal shear strength of a column can be calculated from

$$V_{n,\mathrm{TS500}} = V_c + V_s = 0.8\left(0.65 f_{ctd} A_g \left(1 + 0.007\frac{P}{A_g}\right)\right) + \frac{A_v f_y d}{s} \quad (1)$$

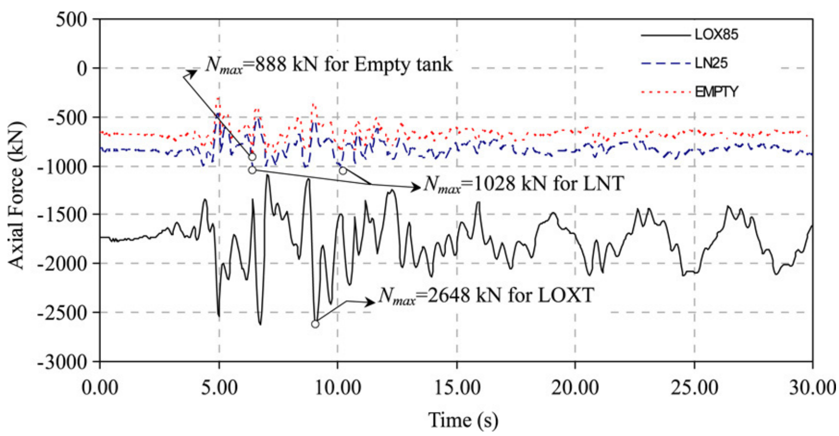

Fig. 9. Calculated time histories of column axial loads for the three tanks analysed.

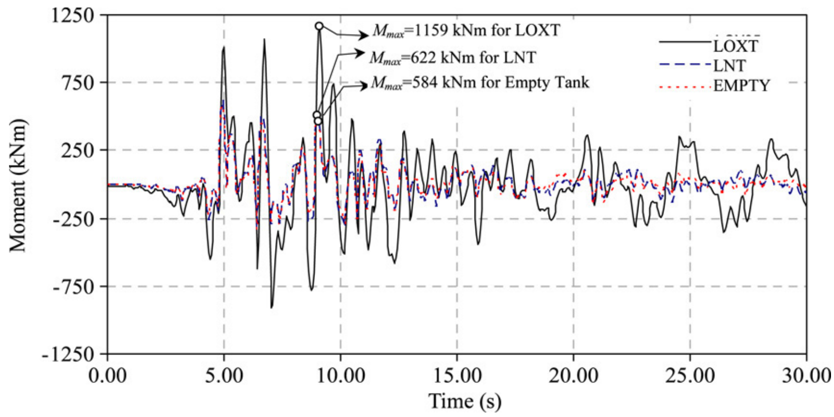

Fig. 10. Calculated time histories of maximum column moments for the three tanks analysed.

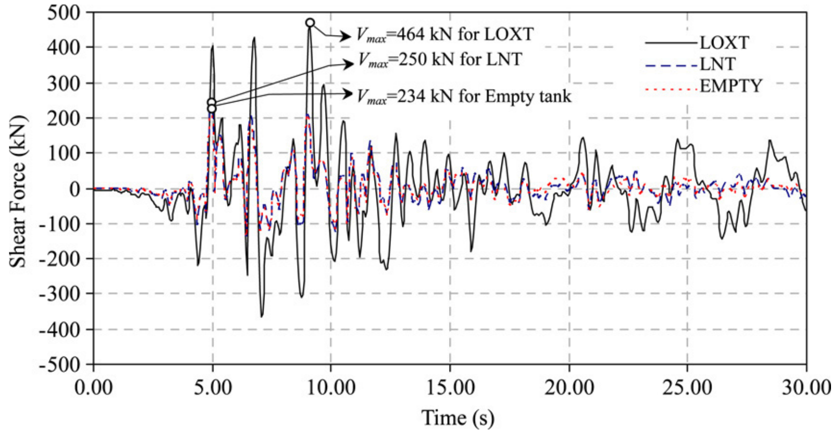

Fig. 11. Calculated time histories of column shear forces for the three tanks analysed

where A_g = gross area of column cross-section, f_{ctd} = design tensile strength of concrete, P = axial load, A_v = transverse reinforcement area within a spacing of s, d = effective depth of section, and f_y = yield strength of transverse reinforcement. It should be noted that mm, N, and MPa units are used in Eq. (1). For a typical 500 mm diameter tank column, $A_g = 196,350\ \text{mm}^2$, the maximum axial load calculated from time history analysis, $P = 2.648 \times 10^6$ N, $f_{ctd} = 1.35$ MPa, $f'_c = 28$ MPa, $A_v = 100.5\ \text{mm}^2$, $d = 450$ mm, $s = 100$ mm, and $f_y = 365$ MPa. Then, the shear strength calculated from Eq. (1) is 316 kN. The maximum dynamic column shear forces (234 and 250 kN) for the empty and liquefied nitrogen tanks were less than the code design shear strength. However, the maximum seismic column shear force for the liquefied oxygen tank (464 kN) is larger than the shear capacity of columns calculated from TS500, indicating that the observed column failures may be due to insufficient shear strength.

Fig. 12 shows a discretized column cross-section and the lateral load–flexural displacement response calculated using the sectional moment–curvature relations. The axial load–moment interaction diagram for a typical column is presented in Fig. 13. For the moment–curvature and axial load–moment interaction curve calculations, an estimated concrete compressive strength, f'_c of 28 MPa is used for the unconfined concrete representing cover concrete. Per Mander et al. [12], a confined concrete strength of 35 MPa is used for concrete confined by column ties. The yield and tensile strengths of the longitudinal steel were estimated to be 414 MPa and 620 MPa, respectively. Fig. 12 shows that, with increasing axial load, the flexural strength and stiffness increases, and deformation capacity decreases. The maximum displacement demands shown in the same figure, i.e., 23 and 11 mm for the oxygen and nitrogen tanks (from Fig. 7), indicate that the columns supporting the oxygen tanks do not seem to have sufficient deformation capacity under the maximum axial load of 2648 kN.

The comparison of maximum predicted seismic axial load–moment pairs (from Figs. 9 and 10) with the combined axial load and moment capacity indicate that force demands on the columns supporting the liquefied oxygen tanks were extremely large (Fig. 13). The axial load–moment demand pairs shown in Fig. 13 occur at distinct instants of time for the Nitrogen and empty tanks even though they are plotted as simultaneous pairs. Considering that these maximum demands were imposed on the columns only a few times and instantaneously during the earthquake, the demands on the empty and nitrogen tank columns are probably close to the limits of the capacity curve. As shown in Fig. 13, the maximum moment, M_p corresponding to the initial gravity load of 1761 kN is 451 kN m. Assuming fixity at the top and bottom of the column, the corresponding shear force V_p is 361 kN or 20% of the supported weight. Assuming that the fluid in the 85% full liquefied oxygen tank was 100% reactive, then the

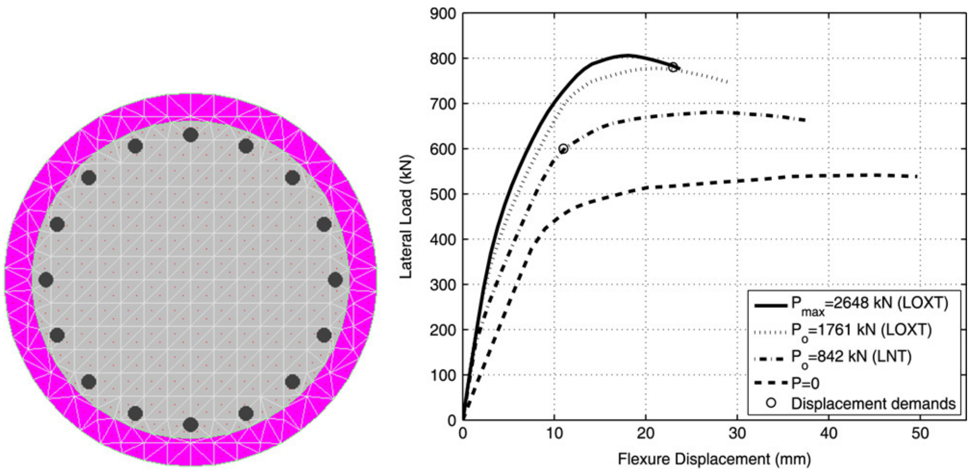

(a) (b)

Fig. 12. (a) fiber cross-section model, and (b) flexural response of columns under different axial loads and the corresponding maximum calculated dynamic displacements.

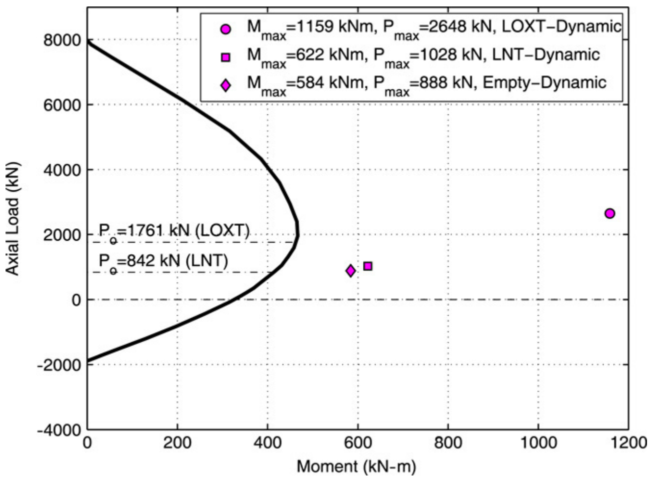

Fig. 13. Axial load–moment interaction diagram for a typical column.

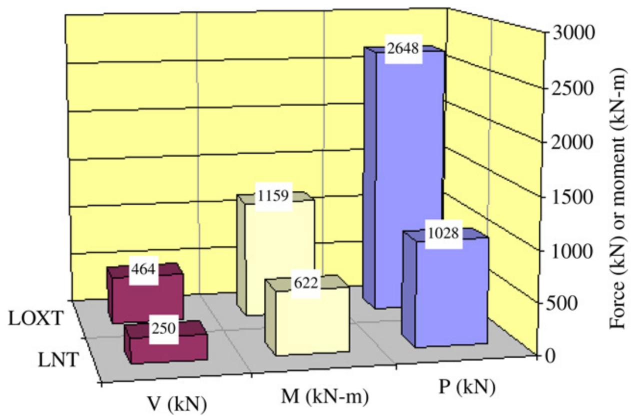

Fig. 14. Comparison of maximum dynamic internal forces for the liquefied Oxygen tank (LOXT) and liquefied Nitrogen tank (LNT).

peak ground acceleration required to fail the columns is $0.20g$. The peak ground acceleration for the input motion (YPT-NS in Table 1) used in the dynamic analysis was $0.32g$. This is probably why the calculated demands are much larger than the capacities shown in Fig. 13. Considering also that the predicted shear force V_p and the shear strength V_n are relatively close, the columns would fail in shear before reaching the maximum flexural strength.

The maximum column internal forces obtained from dynamic analysis are presented in Fig. 14. The data clearly shows that the seismic column moment and shear demands for the liquefied oxygen tanks are roughly two times larger than those for the liquefied nitrogen tank. Similarly, the increase in the predicted maximum axial load is almost 260%. It appears from Fig. 15 that during the earthquake, primarily due to overturning effects, the increase in the axial load was significantly larger for the heavier tanks (LOXT) than for the lighter tank (LNT), i.e. the axial load increase was 887 kN or 50% for LOXT, and 186 kN or 22% for LNT. Undoubtedly, the calculated maximum column axial loads would be different if the vertical component of the strong ground motion (Fig. 2) was included in the dynamic analysis. Similarly, if all three components of the input ground motion were to be included in the dynamic analysis, the results presented in this study would be somewhat different.

6. Simplified model and dynamic analysis of tanks

Quite a few simplified procedures are available for the analysis of elevated tanks including the effects of fluid–structure interaction [11]. Simple two-lumped-mass models are commonly used to analyse the elevated tanks supported by structural frames or columns as in this study. In traditional two-lumped-mass models, the mass of the empty vessel, mass of part of the supporting structure and impulsive mass of the fluid are usually represented by a single lumped-mass, and the convective mass of the fluid is represented by a second lumped-mass (Fig. 16). In addition to these typical masses, the Habas tanks include a heavy reinforced concrete slab right above the support columns. As a result, a modified version of the two-lumped-mass model is developed and used here to analyze the tanks and to compare the results from the

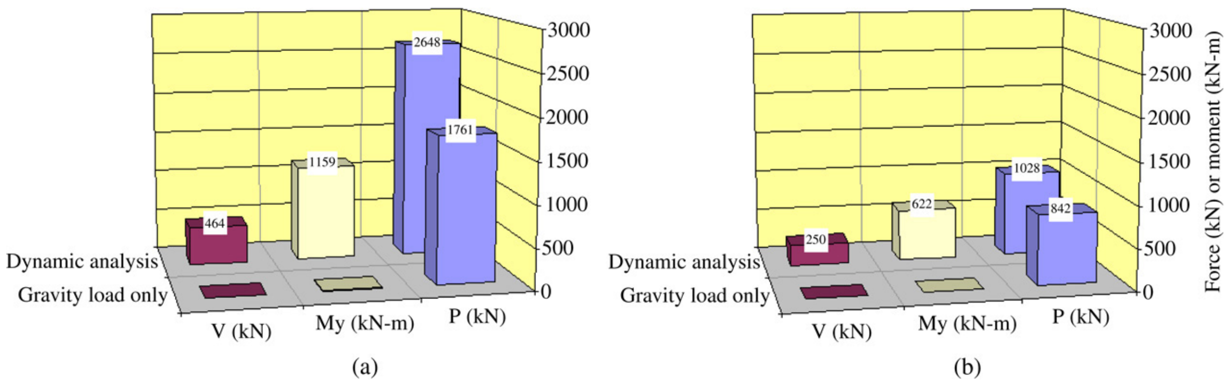

Fig. 15. Comparison of maximum seismic internal forces and initial axial load for: (a) liquefied Oxygen tank (LOXT), and (b) liquefied Nitrogen tank (LNT).

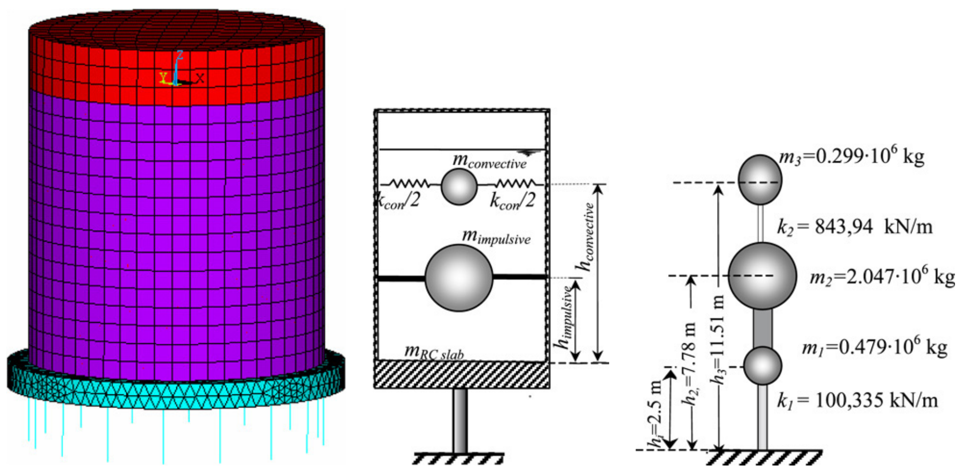

(a) Finite element model. (b) Mechanical model. (c) Simplified model.

Fig. 16. Finite element model and simplified three-lumped-mass model for LOXT.

finite element dynamic analyses discussed above. The proposed simplified three-lumped-mass model is shown in Fig. 16(c). In this model, m_1 is the sum of the masses of rigid concrete slab and support columns; m_2 is the sum of the masses of empty vessel and impulsive mass of the liquefied gas; and m_2 is equal to convective mass of the liquefied gas. k_1 and k_2 are the flexural stiffness of the columns and stiffness of convective mass. It is assumed that the concrete slab and impulsive mass are rigidly connected. Additional information and definition of these parameters are provided in Livaoglu and Dogangun [11].

The shear force time history of a column supporting the liquefied oxygen tank is calculated using the simplified three-lumped-mass model (Fig. 17). The maximum shear force predicted from the simplified model is 650 kN, which is larger than the shear force of 464 kN calculated using the finite element model of the same tank. These results suggest that such a simplified model can be used conservatively in preliminary design or analysis of this type of tanks.

7. Conclusions

During the 1999 Kocaeli, Turkey earthquake, two of the three above-ground tanks located at the Habas plant collapsed as a result of failure of reinforced concrete columns supporting the tanks. The collapsed tanks contained liquefied oxygen and were 85% full, and the undamaged liquefied nitrogen tank was 25% full at the time of the earthquake. The main objective of this study was to analyse the tanks using a finite element model including liquefied gas–structure interaction and a simplified model, and to compare the calculated response with the observed performance. A ground acceleration record from a nearby site, with a peak ground acceleration of 0.32g (YPT-NS), is used as an input motion for the dynamic analysis. The demands calculated from dynamic analyses are compared with the predicted capacities of the support columns. The following are the key conclusions.

The vertical gap between the tank roof and the top level of liquefied Oxygen was sufficiently large such that the sloshing fluid did not affect the roof during the earthquake. When the effect of liquefied gas sloshing is ignored, i.e. if the fluid is modelled as a single rigid mass, the lateral deformations and column internal forces including shear and bending moments are overestimated.

The lateral displacements calculated from dynamic analysis of tanks showed that almost all lateral deformations take place within the 2.5 m high support columns as the tank itself is relatively rigid. If an elevated tank is desired in a seismic

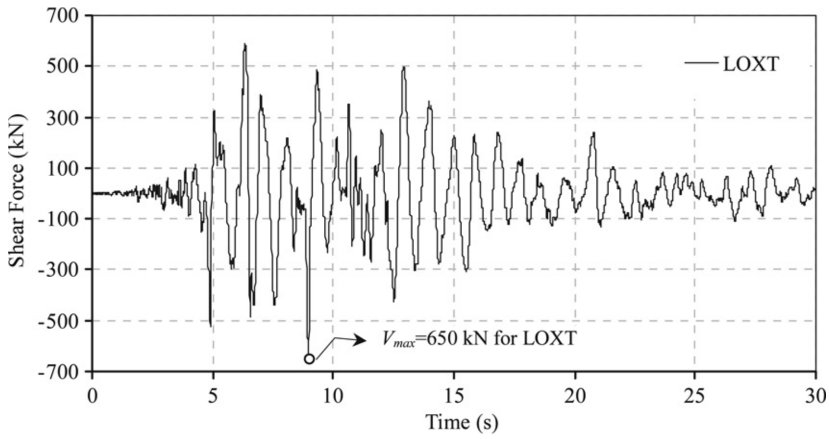

Fig. 17. Dynamic column shear force history calculated using the simplified model for LOXT.

region, the strength and deformation capacity or length of the columns should be increased significantly, or an alternative support structure should be used. The comparison of maximum displacement demands and deformation capacities indicated that the columns supporting the oxygen tanks did not seem to have sufficient deformation capacity under the maximum potential axial load.

The predicted maximum dynamic force demands, including axial load, shear and moments, in columns supporting the collapsed liquefied oxygen tanks were almost two times larger than those in columns of empty and liquefied nitrogen tanks. The estimated shear capacities were larger than the maximum dynamic shear forces in columns supporting the empty and liquefied nitrogen tanks, whereas the column shear strengths were smaller than the maximum dynamic shear demands for the liquefied oxygen tanks, indicating that the observed column failures were also due to insufficient shear strength.

Dynamic analysis of the tanks is repeated using a simplified three-lumped-mass model. The simplified model overestimated the response.

References

[1] ANSYS. V. 10.0. Swanson analysis systems Inc. Houston (Pennsylvania, USA); 2006.
[2] ASCE. Guidelines for seismic evaluation and design of petrochemical facilities. Task committee on seismic evaluation and design of petrochemical facilities. Reston (Virginia): American Society of Civil Engineers; 1997.
[3] Bauer HF. Fluid oscillations in the containers of a space vehicle and their influence upon stability. NASA TRR 187; 1964.
[4] Dogangun A, Livaoglu R. Hydrodynamic pressures acting on the walls of rectangular fluid containers. Structural Engineering and Mechanics 2004; 17(2):203–14.
[5] Eurocode-8. Design of structures for earthquake resistance — Part 4: Silos, tanks, and pipelines. Final PT Draft. European Committee for Standardization; 2003.
[6] FEMA 368. NEHRP Recommended provisions for seismic regulations for new buildings and other structures. Federal emergency management agency; 2001.
[7] Housner GW. Dynamic behavior of water tanks. Bulletin of Seismological Society of the America 1963;53:381–7.
[8] Johnson GH, Aschheim M, Sezen H. Industrial facilities. Kocaeli, Turkey earthquake of August 17, 1999 reconnaissance report, earthquake spectra, supplement A to 16; 2000. p. 311–50.
[9] Huang W, Gould PL, Martinez R, Johnson GS. Non-linear analysis of a collapsed reinforced concrete chimney. Earthquake Engineering and Strucural Dynamics 2004;33:485–98.
[10] Kilic AS, Sozen MA. Evaluation of effect of August 17, 1999, Marmara earthquake on two tall reinforced concrete chimneys. ACI Structural Journal 2003;100(3):357–64.
[11] Livaoglu R, Dogangun A. Simplified seismic analysis procedures for elevated tanks considering fluid–structure-soil interaction. Journal of Fluids and Structures 2006;22(3):421–39.
[12] Mander JB, Priestley MJN, Park R. Theoretical stress–strain model for confined concrete. ASCE Journal of Structural Engineering 1988;114(8): 241–69.
[13] Rahnama M, Morrow G. Performance of industrial facilities in the August 17, 1999, Izmit earthquake. In: Proc., 12th world conf. on earthquake engineering; 2000.
[14] Sezen H, Elwood KJ, Whittaker AS, Mosalam KM, Wallace JW, Stanton JF. Structural engineering reconnaissance of the August 17, 1999 Kocaeli (Izmit), Turkey Earthquake. PEER rep. no. 2000/09. Pacific Earthquake Engineering Research Center, University of California; 2000. http://nisee.berkeley.edu/turkey/.
[15] Sezen H, Whittaker AS. Seismic performance of industrial facilities affected by the 1999 Turkey earthquake. ASCE Journal of Performance of Constructed Facilities 2006;20(1):28–36.
[16] Sezen H, Whittaker AS, Elwood KJ, Mosalam KM. Performance of reinforced concrete and wall buildings during the August 17, 1999 Kocaeli, Turkey earthquake, and seismic design and construction practice in Turkey. Engineering Structures 2003;25(1):103–14.
[17] TS 500. Requirements for design and construction of reinforced concrete structures. Ankara: Turkish Standards Institute; 2000.
[18] Turkish Seismic Code. Specification for structures to be built in disaster areas; Part III–Earthquake disaster prevention. Ministry of Public Works and Settlement, Government of the Republic of Turkey; 1998.
[19] UBC. International conference of building officials. Uniform building code, vol. 2: Structural engineering design provisions. Whittier (California); 1997.